J|A|C|S
ARTICLES
Published on Web 12/06/2006

# Control of Interchain Contacts, Solid-State Fluorescence Quantum Yield, and Charge Transport of Cationic Conjugated Polyelectrolytes by Choice of Anion

Renqiang Yang, Andres Garcia, Dmitry Korystov, Alexander Mikhailovsky, Guillermo C. Bazan,* and Thuc-Quyen Nguyen*

*Contribution from the Mitsubishi Chemical Center for Advanced Materials, Department of Chemistry & Biochemistry, Institute for Polymers and Organic Solids, University of California, Santa Barbara, California 93106*

Received February 17, 2006; E-mail: bazan@chem.ucsb.edu; quyen@chem.ucsb.edu

***Abstract:*** Simple procedures are provided for exchanging charge-compensating ions in conjugated polyelectrolytes by progressive dilution of the original species and for determining the degree of ion exchange by using X-ray photoelectron spectroscopy. By using these methods, the bromide ions in poly[(9,9-bis(6′-*N*,*N*,*N*-trimethylammoniumbromide)hexyl)fluorene-*co*-*alt*-4,7-(2,1,3-benzothiadiazole)] were exchanged with $BF_4^-$, $CF_3SO_3^-$, $PF_6^-$, $BPh_4^-$, and $B(3,5\text{-}(CF_3)_2C_6H_3)_4^-$ ($BAr^F{}_4^-$). Absorption, photoluminescence (PL), and PL quantum yields ($\Phi$) were measured in different solvents and in solid films cast from methanol. Examination of the resulting trends, together with the spectral bandshapes in different solvents, suggests that increasing the counteranion (CA) size decreases interchain contacts and aggregation and leads to a substantial increase of $\Phi$ in the bulk. Size analysis of polymers containing $Br^-$ and $BAr^F{}_4^-$ in water by dynamic light scattering techniques indicates suppression of aggregation by $BAr^F{}_4^-$. Nanoscale current-voltage measurements of films using conducting atomic force microscopy show that hole mobilities and, more significantly, charge injection barriers are CA dependent. These results show that it is possible to significantly modify the optoelectronic properties of conjugated polyelectrolytes by choosing different counterions. A parent conjugated backbone can thus be fine-tuned for specific applications.

## Introduction

Conjugated polyelectrolytes (CPs) are polymers characterized by a $\pi$-conjugated backbone and functional groups that ionize in high dielectric media, thereby making the material soluble in water and polar organic solvents.[1] CPs embody the properties of polyelectrolytes, which are modulated by complex long-range electrostatic interactions,[2] with the useful optical and electronic functions of organic semiconductors, which are determined to a significant extent by chain conformations and interchain contacts.[3] Optical and electronic properties in solution[4] and in the solid state are therefore difficult to predict a priori from simple molecular structure considerations.

Despite their complex structure/property relationships, CPs have found recent applications in substantially different technologies.[5] For example, cationic CPs with a copolymer structure containing fluorene and phenylene repeat units[6] can be used for the optical amplification of fluorescent biosensors.[7] In this function, the conjugated backbone plays a light harvesting role, while the charged groups orchestrate electrostatic interactions as a function of a given recognition event. The presence of charge compensating counterions allows fabrication of light-emitting electrochemical cells (LECs)[8] where the CP provides

(1) Pinto, M. R.; Schanze, K. S. *Synthesis* **2002**, *9*, 1293.
(2) (a) *Polyelectrolytes: Science and Technology*; Hara, M., Ed.; Marcel Dekker: New York, 1993. (b) Bohrisch, J.; Eisenbach, C. D.; Jaeger, W.; Mori, H.; Muller, A. H. E.; Rehahn, M.; Schaller, C.; Traser, S.; Wittmeyer, P. *Adv. Polym. Sci.* **2004**, *165*, 1. (c) Holm, C.; Rehahn, M.; Oppermann, W.; Ballauf, M. *Adv. Polym. Sci.* **2004**, *166*, 1−27.
(3) Hadziioannou, G., van Hutten, P. F., Eds. *Semiconducting Polymers, Chemistry, Physics and Engineering*; Wiley−VCH: New York, 2000.
(4) Wang, S.; Gaylord, B. S.; Bazan, G. C. *J. Am. Chem. Soc.* **2004**, *126*, 5446−5451.
(5) (a) Baur, J. W.; Kim, S.; Balanda, P. B.; Reynolds, J. R.; Rubner, M. F. *Adv. Mater.* **1998**, *10*, 1452. (b) Cimrova, V.; Schmidt, W.; Rulkens, R.; Schulze, M.; Meyer, W.; Neher, D. *Adv. Mater.* **1996**, *8*, 585. (c) Chang, S. C.; Bharathan, J.; Yang, Y.; Helgeson, R.; Wudl, F.; Ramey, M. B.; Reynolds, J. R. *Appl. Phys. Lett.* **1998**, *73*, 2561. (d) Ho, P. K. H.; Kim, J. S.; Burroughes, J. H.; Becker, H.; Li, S. F. Y.; Brown, T. M.; Cacialli, F.; Friend, R. H. *Nature* **2000**, *404*, 481. (e) Ding, L.; Jonforsen, M.; Roman, L. S.; Andersson, M. R.; Inganäs, O. *Synth. Met.* **2000**, *110*, 133. (f) Zhou, G.; Qian, G.; Ma, L.; Cheng, Y. X.; Xie, Z. Y.; Wang, L. X.; Jing, X. B.; Wang, F. S. *Macromolecules* **2005**, *38*, 5416. (g) Argun, A. A.; Aubert, P. H.; Thompson, B. C.; Schwendeman, I.; Gaupp, C. L.; Hwang, J.; Pinto, N. J.; Tanner, D. B.; MacDiarmid, A. G.; Reynolds, J. R. *Chem. Mater.* **2004**, *16*, 4401. (h) Achyuthan, K. E.; Bergstedt, T. S.; Chen, L.; Jones, R. M.; Kumaraswamy, S.; Kushon, S. A.; Ley, K. D.; Lu, L.; McBranch, D.; Mukundan, H.; Rininsland, F.; Shi, X.; Xia, W.; Whitten, D. G. *J. Mater. Chem.* **2005**, *15*, 2648. (i) Xue, C.; Chen, Z.; Luo, F.-T.; Palaniappan, K.; Chesney, D. J.; Liu, J.; Chen, J.; Liu, H. *Biomacromolecules* **2005**, *6*, 1810. (j) Wosnick, J. H.; Mello, C. M.; Swager, T. M. *J. Am. Chem. Soc.* **2005**, *127*, 3400. (k) Herland, A.; Nilsson, K. P. R.; Olsson, J. D. M.; Hammarstrom, P.; Konradsson, P.; Inganas, O. *J. Am. Chem. Soc.* **2005**, *127*, 2317. (l) Huang, F.; Hou, L.; Wu, H.; Wang, X.; Shen, H.; Cao, W.; Yang, W.; Cao, Y. *J. Am. Chem. Soc.* **2004**, *126*, 9845. (m) An, L.; Tang, Y.; Wang, S.; Li, Y.; Zhu, D. *Macromol. Rapid Commun.* **2006**, *27*, 993.
(6) Stork, M.; Gaylord, B. S.; Heeger, A. J.; Bazan, G. C. *Adv. Mater.* **2002**, *14*, 361.
(7) (a) Liu, B.; Gaylord, B. S.; Wang, S.; Bazan, G. C. *J. Am. Chem. Soc.* **2003**, *125*, 6705. (b) Liu, B.; Bazan, G. C. *Proc. Natl. Acad. Sci. U.S.A.* **2005**, *102*, 589. (c) Gaylord, B. S.; Heeger, A. J.; Bazan, G. C. *Proc. Natl. Acad. Sci. U.S.A.* **2002**, *99*, 10954.
(8) (a) Pei, Q.; Yu, G.; Zhang, C.; Yang, Y.; Heeger, A. J. *Science* **1995**, *269*, 1086. (b) Pei, Q.; Yang, Y.; Yu, G.; Zhang, C.; Heeger, A. J. *J. Am. Chem. Soc.* **1996**, *118*, 3922.


**10.1021/ja0611341 CCC: $33.50** 

***Scheme 1.*** Chemical Structures and Synthetic Entry into Polymers of the Type **PFBT-X**[a]

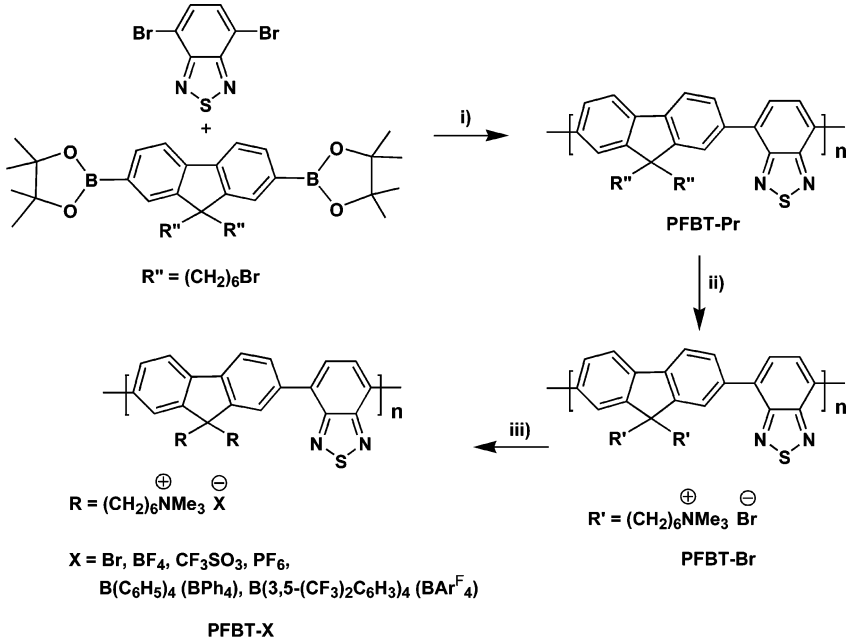


[a] Conditions: (i) $Pd(PPh_3)_4/Na_2CO_3$, toluene; (ii) $NMe_3$, THF, $H_2O$; (iii) MX, M = $Na^+$ or $NH_4^+$, $H_2O$.

a single component material that incorporates electrochemical (including charge compensating ions)[9] and emissive functions,[10] thereby circumventing the need to design and stabilize multicomponent blends. Because of their solubility in polar solvents, it is possible to use CPs in combination with neutral, organic soluble, conjugated polymers to fabricate multilayer polymer light emitting diodes by spin-coating techniques.[11] In the last application, the CPs have been used as electron or hole transport materials, because their solid-state emission quantum yields are typically low and are not likely to function well as the emitting layer.

Chain conformations and interchain association in solution can influence device functions that depend strongly on the extent of electronic delocalization in individual chains and on the collective interchain packing of conjugated polymers.[12] Relevant to the discussion here is that work on non-conjugated polyelectrolytes has demonstrated that the nature of the counterions influences macromolecular conformations, interchain repulsion, solubility, polyion dimensions, and stability.[13] A similar level of understanding is not available in the case of CPs[14] and in particular on how optoelectronic performance may be controlled in different media by properties of the counterion such as size, hydrophobicity, mobility, redox potential, and charge density.

To address the concerns above, we provide in this contribution a straightforward anion exchange method and characterization procedure for determination of exchange efficiency. We take advantage of the resulting materials to examine how different counteranions (CAs) affect the solid-state photoluminescence (PL) quantum yields, the nanoscale charge transport properties, and the aggregation of the chains in solution. We will take advantage of a typical cationic CP framework, poly[(9,9-bis(6′-*N*,*N*,*N*-trimethylammonium)hexyl)fluorene-*alt*-4,7-(2,1,3-benzothiadiazole)] (**PFBT-X**, where **X** corresponds to the charge compensating anion, see Scheme 1), as the subject of our studies. The specific polymer bearing bromide counteranions (**PFBT-Br**) recently found use in the optical amplification of fluorescent DNA microarrays used in DNA-chip technologies.[7b] While **PFBT-Br** has been reported previously, the observations of substantial perturbations by different CAs are likely to be general and should be taken into consideration in the future design and applications of conjugated polyelectrolytes.

## Results and Discussion

**Synthesis and Characterization.** The synthesis of **PFBT** is available in the literature.[7b] Briefly, the polymerization sequence relies on palladium-mediated Suzuki cross-coupling copolymerization of 2,7-bis[9,9-bis(6-bromohexyl)-fluorenyl]-4,4,5,5-tetramethyl-[1.3.2]dioxaborolane and 4,7-dibromo-2,1,3-benzothiadiazole to give the precursor material poly[9,9-bis(6-bromohexyl)fluorene-*alt*-4,7-(2,1,3-benzothiadiazole)] (**PFBT-Pr**) in 60−70% isolated yields (Scheme 1). Quaternization of the pendent hexylbromide groups in **PFBT-Pr** using trimethylamine yields **PFBT-Br**. Bromide exchange can be accomplished by dissolving **PFBT-Br** in a methanol and water solution containing an excess of a salt with the CA of interest. The solvent is then removed under reduced pressure, and the resulting solid is washed several times with deionized water.

(9) Cao, Y.; Pei, Q.; Andersson, M. R.; Yu, G.; Heeger, A. J. *J. Electrochem. Soc.* **1998**, *144*, L317.
(10) (a) Edman, L.; Pauchard, M.; Liu, B.; Bazan, G.; Moses, D.; Heeger, A. J. *Appl. Phys. Lett.* **2003**, *82*, 3961. (b) Edman, L.; Liu, B.; Vehse, M.; Swensen, J.; Bazan, G. C.; Heeger, A. J. *J. Appl. Phys.* **2005**, *98*, 44502.
(11) (a) Ramey, M. B.; Hiller, J.; Rubner, M. F.; Tan, C.; Schanze, K. S.; Reynolds, J. R. *Macromolecules* **2005**, *38*, 234. (b) Ma, W.; Iyer, P. K.; Gong, X.; Liu, B.; Moses, D.; Bazan, G. C.; Heeger, A. J. *Adv. Mater.* **2005**, *17*, 274. (c) Gong, X.; Wang, S.; Moses, D.; Bazan, G. C.; Heeger, A. J. *Adv. Mater.* **2005**, *17*, 2053. (d) Meerholz, K. *Nature* **2005**, *437*, 327.
(12) (a) Nguyen, T.-Q.; Martini, I. B.; Liu, J.; Schwartz, B. J. *J. Phys. Chem. B* **2000**, *104*, 237. (b) Nguyen, T.-Q.; Doan, V.; Schwartz, B. J. *J. Chem. Phys.* **1999**, *110*, 4068. (c) Jakubiak, R.; Collison, C. J.; Wan, W. C.; Rothberg, L. J.; Hsieh, B. R. *J. Phys. Chem. A* **1999**, *103*, 2394.
(13) Such as: (a) Dubois, E.; Boue, F. *Macromolecules* **2001**, *34*, 3684. (b) Singh, S. K.; Caram-Lelham, N. *J. Colloid Interface Sci.* **1998**, *203*, 430. (c) Benegas, J. C.; Paoletti, S.; Hoop, M. A. G. T. *Macromol. Theory Simul.* **1999**, *8*, 61. (d) Zhang, Y.; Douglas, J. F.; Ermi, B. D.; Amis, E. J. *J. Chem. Phys.* **2001**, *114*, 3299. (e) Hinderberger, D.; Spiess, H. W.; Jeschke, G. *J. Phys. Chem. B* **2004**, *108*, 3698. (f) Combet, J.; Isel, F.; Rawiso, M.; Boue, F. *Macromolecules* **2005**, *38*, 7456.
(14) Hammond, P. T. *Curr. Opin. Colloid Interface Sci.* **2000**, *4*, 430.

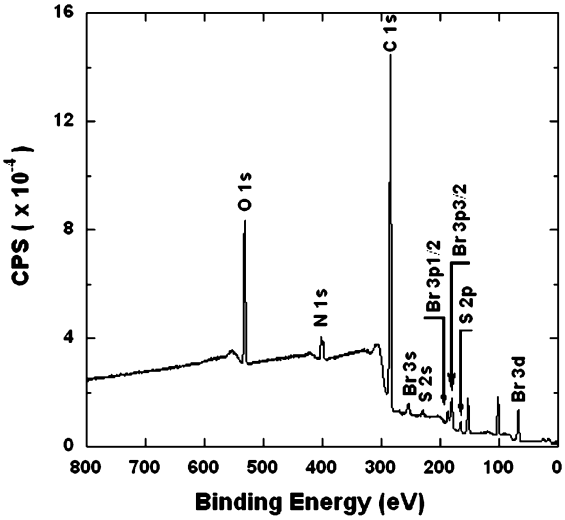


***Figure 1.*** XPS analysis of **PFBT-Br**.

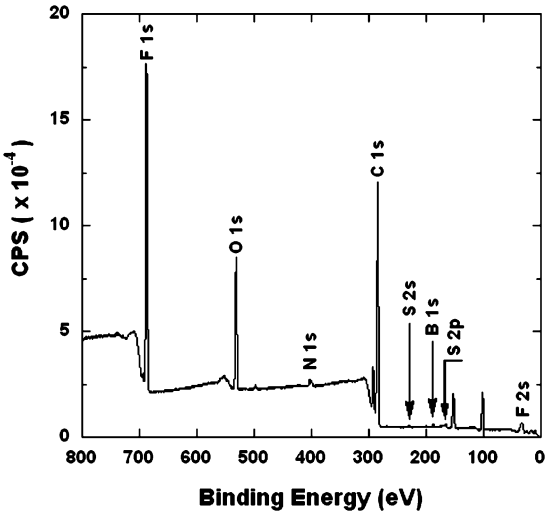


***Figure 2.*** XPS analysis of **PFBT-BAr$^F_4$**.

The overall procedure is repeated until the majority of the bromide originally present in **PFBT-Br** is removed.

Analysis of **PFBT-X** powders by X-ray photoelectron spectroscopy (XPS) confirms greater than 95% bromide exchange. As shown in Figure 1, the parent **PFBT-Br** displays four peaks characteristic of $Br^-$ (Br3d, $Br3p_{3/2}$, $Br3p_{1/2}$, and Br3s at binding energies (BEs) of 69, 182, 189, and 257 eV, respectively).[15] In the case of **PFBT-BAr$^F_4$** (where $BAr^F_4$ = $B(3,5\text{-}(CF_3)_2C_6H_3)_4^-$), the bromide peaks are replaced by signals corresponding to F (F1s and F2s at 687 and 31 eV, respectively) and B (B1s at 188 eV); see Figure 2. Similarly, for **PFBT-BF$_4$**, new peaks appear that can be traced to the presence of F (686 and 30 eV) and B (192 eV). Characterization of **PFBT** with other CAs and the method for calculating atomic concentration ratios can be found in the Supporting Information. XPS is thus a convenient method for elemental composition determination, an important piece of information to obtain reliable structure/property relationships.

**Absorption and Photoluminescence (PL) Spectroscopy.** Absorption and PL spectra of **PFBT** with different CAs in dimethylsulfoxide (DMSO), methanol (MeOH), deionized water, and in the solid state are summarized in Table 1. Measurements in DMSO as a function of CA provide the narrowest range of absorption maxima ($\lambda_{abs} \approx 450-455$ nm; $\Delta\lambda_{max} = 5$ nm) and PL maxima ($\lambda_{PL} \approx 569-572$ nm; $\Delta\lambda_{PL} = 3$ nm). PL quantum yields ($\Phi$), determined by comparison with emission standards in the same solvent, range from 35% (Br) to 45% ($BAr^F_4$). These values are quite similar, given the statistical uncertainties that arise from errors in $\Phi$ determination ($\pm$5%). The polymers show considerably higher solubility in DMSO, relative to MeOH and water. Spectroscopic measurements in DMSO thus provide an average picture that is more biased toward poorly interacting chains.

The CAs make a more substantial influence on the absorbance and emission properties in water, relative to DMSO, as shown by the larger values of $\Delta\lambda_{abs}$ (14 nm) and $\Delta\lambda_{PL}$ (20 nm) and the larger $\Phi$ range, from 3% (**PFBT-Br**) to 22% (**PFBT-BAr$^F_4$**). In methanol, the changes in optical properties more closely resemble those in DMSO than in water and are provided in Table 1 for comparison with the properties measured in films spun-cast from methanol.

Trends similar to those observed in water are observed in the films, with $\Delta\lambda_{abs} = 18$ nm and $\Delta\lambda_{PL} = 18$ nm. More pronounced changes occur in the $\Phi$'s of the films, where values span from 5% (**PFBT-Br**) to 41% (**PFBT-BAr$^F_4$**). These solid-state measurements involved examination of films spun from methanol, optical excitation at 364 nm, and collection of emission using an integrating sphere.[16] That the data in water and in the solid show similar trends is consistent with significant aggregation in solution as a result of the hydrophobic nature of the $\pi$-delocalized backbone and emission self-quenching by virtue of the increased interchain contacts.[17] The $\Phi$ of **PFBT-BAr$^F_4$** films is the highest value reported for a CP and is competitive with the efficiencies of neutral conjugated polymers.[16a,18] There is therefore no intrinsic reason why CPs cannot serve as the emitting layer in polymer light emitting diodes.[19] This excellent efficiency also provides strong motivation for exploring different CAs with a given CP for increasing the light output of LECs.

It is informative to examine the spectral features observed with the two CAs ($Br^-$ and $BAr^F_4{}^-$) that give rise to the largest difference in $\Phi$ values (Figure 3). Focusing on the film, one observes that the absorption spectrum is considerably broader for **PFBT-Br**, relative to **PFBT-BAr$^F_4$**. We suggest that the smaller size of $Br^-$ allows for more intimate interchain contacts, a broader distribution of sites, and increased self-quenching. Consistent with this proposal is that the solid state $\Phi$'s in Table 1 roughly track with the CA size, with the largest anions providing more efficient emission. In the aqueous aggregates, where interchain contacts are known to lead to PL self-

(15) Moulder, J. F.; Stickle, W. F.; Sobol, P. E.; Bomben, K. D. *Handbook of X-Ray Photoelectron Spectroscopy*; Physical Electronics, Inc.: MN, 1995.

(16) (a) Greenham, N. C.; Samuel, I. D. W.; Hayes, G. R.; Phillips, R. T.; Kessener, Y. A. R. R.; Moratti, S. C.; Holmes, A. B.; Friend, R. H. *Chem. Phys. Lett.* **1995**, *241*, 89. (b) deMello, J. C.; Wittmann, H. F.; Friend, R. H. *Adv. Mater.* **1997**, *9*, 230.

(17) Gaylord, B. S.; Heeger, A. J.; Bazan, G. C. *J. Am. Chem. Soc.* **2003**, *125*, 896.

(18) (a) Remmers, M.; Neher, D.; Gruner, J.; Friend, R. H.; Gelinck, G.; Warman, J. M.; Quattrocchi, C.; Santos, D. A.; Bredas, J.-L. *Macromolecules* **1996**, *29*, 7432. (b) Tasch, S.; List, E. J. W.; Hochfilzer, C.; Leising, G.; Schlichting, P.; Rohr, U.; Geerts, Y.; Scherf, U.; Mullen, K. *Phys. Rev. B* **1997**, *56*, 4479. (c) Yu, W.-L.; Pei, J.; Cao, Y.; Huang, W.; Heeger, A. J. *Chem. Commun.* **1999**, 1837. (d) Samuel, I. D. W.; Crystall, B.; Rumbles, G.; Burn, P. L.; Holmes, A. B.; Friend, R. H. *Chem. Phys. Lett.* **1993**, *213*, 472.

(19) Burroughes, J. H.; Bradley, D. D. C.; Brown, A. R.; Marks, R. N.; MacKay, K.; Friend, R. H.; Burns, P. L.; Holmes, A. B. *Nature* **1990**, *347*, 539.

***Table 1.*** Summary of Absorption, PL, and Φ Information of **PFBT-X** Solutions and Films

| | DMSO | | | MeOH | | | $H_2O$ | | | film[a] | | |
|---|---|---|---|---|---|---|---|---|---|---|---|---|
| | UV | PL | | UV | PL | | UV | PL | | UV | PL | |
| CA | $\lambda_{abs}$ (nm) | $\lambda_{PL}$ (nm) | Φ (%) | $\lambda_{abs}$ (nm) | $\lambda_{PL}$ (nm) | Φ (%) | $\lambda_{abs}$ (nm) | $\lambda_{PL}$ (nm) | Φ (%) | $\lambda_{abs}$ (nm) | $\lambda_{PL}$ (nm) | Φ (%) |
| Br | 450 | 570 | 35 | 446 | 568 | 29 | 435 | 589 | 3 | 467 | 574 | 5 |
| $BF_4$ | 454 | 572 | 39 | 444 | 562 | 31 | 441 | 592 | 4 | 449 | 570 | 8 |
| $CF_3SO_3$ | 455 | 572 | 43 | 451 | 565 | 34 | 442 | 576 | 5 | 463 | 578 | 12 |
| $PF_6$ | 450 | 572 | 43 | 443 | 564 | 29 | 439 | 588 | 6 | 449 | 574 | 11 |
| $BPh_4$ | 451 | 569 | 34 | 449 | 568 | 28 | 446 | 577 | 9 | 460 | 570 | 15 |
| $BAr^F{}_4$ | 455 | 570 | 45 | 450 | 563 | 36 | 449 | 572 | 22 | 457 | 560 | 41 |

[a] Films were spun-cast from MeOH solution.

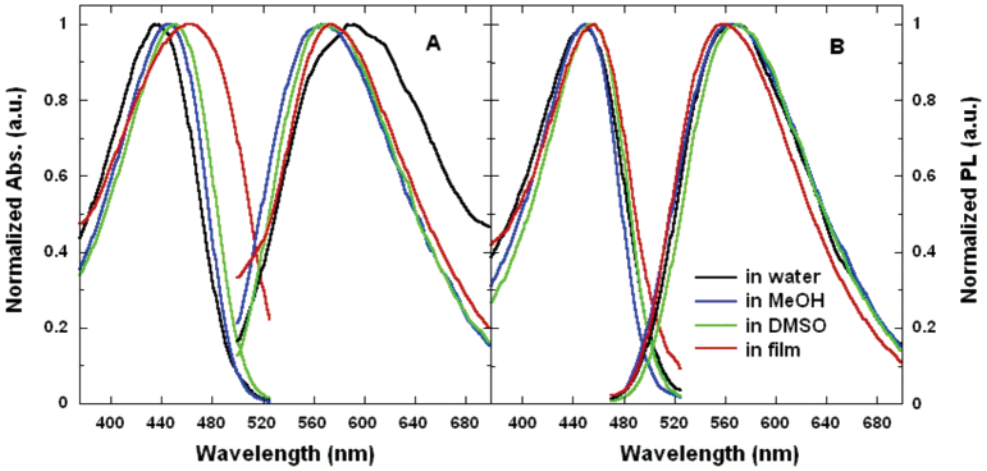


***Figure 3.*** Absorption and PL spectra in water, MeOH, DMSO, and in films of (a) **PFBT-Br** and (b) **PFBT-BAr$^F{}_4$**.

quenching,[6] a similar phenomenon can be invoked, with the larger CAs providing "spacers" that separate polymer chains more effectively.[12,20] By taking advantage of these CAs to increase Φ in water, one should be able to increase the sensitivity of assays used to determine the concentration of DNA.[21]

Comparison of the absorbance and PL peak shapes of **PFBT-Br** and **PFBT-BAr$^F{}_4$** shows that the larger anion also makes the spectra less sensitive to the solvent. This lower sensitivity suggests that most spectral changes are induced by interchain contacts, rather than medium polarity and/or hydrogen-bonding ability (in the case of the films, the polymer itself behaves as the solvent). Such behavior was surprising to us in view of electronic structure calculations for the uncharged analogue of PFBT, which indicate a LUMO localized on the BT units and a charge redistribution upon excitation, features that should give rise to solvatochromism.[22]

**Aggregation in Solution.** As mentioned previously, the coil conformation and the aggregation of conjugated polymers in solution often influence the distribution of chains in spun-cast films.[23] The presence of aggregates in conjugated polymers has been studied extensively and is known to increase fluorescence quenching and facilitate interchain charge transfer and thus charge mobility in the solid.[12,24] For CPs in a polar medium, the chains presumably come together and aggregate to minimize exposure of the hydrophobic π-conjugated backbone.[25] Even in the case of well-defined charged oligomers, one obtains aggregates that incorporate hundreds of molecules, even at low concentrations.[26]

With the considerations described in the preceding paragraph in mind, dynamic light scattering experiments in water were performed with the CAs that provide for the largest changes of the optical properties in Table 1. These studies, carried out over the concentration range from $1.2 \times 10^{-5}$ to $6.3 \times 10^{-6}$ M, gave effective diameters of 353 nm for **PFBT-Br** and 73 nm for **PFBT-BAr$^F{}_4$**. Considering the increase in the mass of the repeat unit from $Br^-$ (742 g/mol) to $BAr^F{}_4{}^-$ (2308 g/mol), one would expect larger dimensions with **PFBT-BAr$^F{}_4$**. A comparison of the greater than 3-fold anticipated molecular weight increase to the decrease in particle size obtained by light scattering provides strong support for reduced aggregation of **PFBT-BAr$^F{}_4$**, relative to **PFBT-Br**. One possible explanation is that electrostatic association of the large $BAr^F{}_4{}^-$ with the backbone

(20) Tan, C.; Atas, E.; Muller, J. G.; Pinto, M. R.; Kleiman, V. D.; Schanze, K. S. *J. Am. Chem. Soc.* **2004**, *126*, 13685.
(21) Hong, J. W.; Henme, W. L.; Keller, G. E.; Rinke, M. T.; Bazan, G. C. *Adv. Mater.* **2006**, *18*, 878.
(22) Cornil, J.; Gueli, I.; Dkhissi, A.; Sancho-Garcia, J. C.; Hennebicq, E.; Calbert, J. P.; Lemaur, V.; Beljonne, D.; Bredas, J. L. *J. Chem. Phys.* **2003**, *118*, 6615.
(23) (a) Nguyen, T.-Q.; Yee, R. Y.; Schwartz, B. J. *J. Photochem. Photobiol., A* **2001**, *144*, 21. (b) Nguyen, T.-Q.; Kwong, R. C.; Thompson, M. E.; Schwartz, B. J. *Appl. Phys. Lett.* **2000**, *76*, 2454.
(24) (a) Donley, C. L.; Zaumseil, J.; Andreasen, J. W.; Nielsen, M. M.; Sirringhaus, H.; Friend, R. H.; Kim, J.-S. *J. Am. Chem. Soc.* **2005**, *127*, 12890. (b) Moliton, A.; Hiorns, R. C. *Polym. Int.* **2004**, *53*, 1397. (c) Collison, C. J.; Treemaneekarn, V.; Oldham, W. J.; Hsu, J. H.; Rothberg, L. J. *Synth. Met.* **2001**, *119*, 515.
(25) (a) Gu, Z.; Bao, Y.-J.; Zhang, Y.; Wang, M.; Shen, Q.-D. *Macromolecules* **2006**, *39*, 3125. (b) Burrows, H. D.; Lobo, V. M. M.; Pina, J.; Ramos, M. L.; Seixas, de Melo, J.; Valente, A. J. M.; Tapia, M. J.; Pradhan, S.; Scherf, U. *Macromolecules* **2004**, *37*, 7425. (c) Mori, T.; Watanabe, T.; Minagawa, K.; Tanaka, M. *J. Polym. Sci,: Part A: Polym. Chem.* **2005**, *43*, 1569. (d) Chen, B.; Metera, K.; Sleiman, H. F. *Macromolecules* **2005**, *38*, 1084. (e) Jonkheijm, P.; Fransen, M.; Schenning, A. P. H. J.; Meijer, E. W. *J. Chem. Soc., Perkin Trans.* **2001**, *2*, 1280. (f) Schnablegger, H.; Antonietti, M.; Goltner, C.; Hartmann, J.; Colfen, H.; Samori, P.; Rabe, J. P.; Hager, H.; Heitz, W. *J. Colloid Interface Sci.* **1999**, *212*, 24.
(26) Gaylord, B. S.; Wang, S. J.; Heeger, A. J.; Bazan, G. C. *J. Am. Chem. Soc.* **2001**, *123*, 6417.

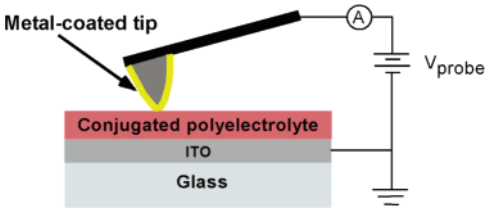


***Figure 4.*** Schematic of the C-AFM experimental setup for characterization of local current versus field characteristics of conjugated polyelectrolyte films.

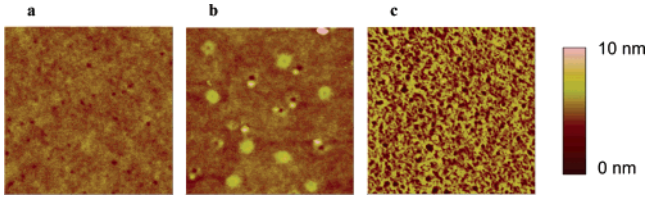


***Figure 5.*** Topography images of films (2.5 $\mu$m × 2.5 $\mu$ m) spun-cast from methanol solutions of (a) **PFBT-Br**, (b) **PFBT-BAr$^F_4$**, and (c) from a toluene solution of **PFBT-Pr**.

inhibits contacts with other chains. Another factor to consider is that interactions of the chain with $BAr^F_4$, with its four aromatic units, may result in backbone−CA hydrophobic interactions that are not possible with $Br^-$.[27] Thus, the driving force for chain packing that minimizes contact with the aqueous surroundings is reduced.

**Charge Transport Measurements.** Atomic force microscopy (AFM) and conducting AFM (C-AFM) were used to examine surface and electronic properties within domains of nanoscalar dimensions. C-AFM is a scanning probe technique, which examines surface topography and local current simultaneously[28] and can provide information on the nanoscale charge transport properties within specific domains. In these measurements, the conducting probe makes contact at different locations of the sample, and a tip acts as a nanoelectrode to measure current as a function of applied voltage. One can thereby obtain $I-V$ curves at different sample locations to examine charge transport heterogeneity at the local level. Such information can be integrated to provide an average for the bulk material. Figure 4 illustrates the test configuration used in our studies. The current measured is expected to be predominantly by hole transport, because the ITO substrate and the Pt tip have work functions of 4.7 and 5.6 eV, respectively, and the polymer HOMO energy is approximately 5.8 eV.[29] Based on consideration of these energies, there is a smaller barrier for hole injection from the Pt tip (∼0.2 eV) than from ITO (1.1 eV).[30]

The effect of CAs on the surface roughness is shown by the AFM images in Figure 5. Films spun-cast from methanol are approximately 20 nm thick and appear smooth and homogeneous, with an rms roughness of 0.4 nm for **PFBT-Br** (Figure 5a). In the case of **PFBT-BAr$^F_4$**, one observes circular topographic features with a diameter of ∼100 nm and a slightly increased roughness (rms ≈ 0.8 nm). As will be discussed later, these topographic features do not influence charge carrier mobility. To obtain smooth **PFBT-BAr$^F_4$** films, one needs to stir the polymer in methanol for extended periods of time, typically overnight. Shorter times lead to films with surfaces with more pronounced roughness. The surfaces of **PFBT-Br** and **PFBT-BAr$^F_4$** are featureless, a typical morphology for amorphous films. The neutral form of this polymer (**PFBT-Pr**) was also studied for a comparison. **PFBT-Pr** films were spun-cast from toluene with thickness similar to those of **PFBT-Br** and **PFBT-BAr$^F_4$**. The surface roughness of **PFBT-Pr** is ∼1.4 nm (Figure 5c), a factor of 3 higher than the charged polymers. Close examination of the **PFBT-Pr** film reveals a morphology containing interpenetrating fibers.

Figure 6a shows the average $I-V$ curves obtained by using C-AFM. In these measurements, the tip/sample contact surface area is ∼84 nm$^2$. The data were collected from five sets of films with 40 $I-V$ curves obtained from each sample. Current is observed in the **PFBT-Br** film in reverse (holes are injected from the ITO) and forward bias (holes are injected from Pt tip), whereas for the **PFBT-BAr$^F_4$** film, current can only be observed in the forward bias. Examination of neutral **PFBT-Pr** reveals a behavior similar to that of **PFBT-BAr$^F_4$**; only forward bias current is observed.

Analysis of the current density ($J$) versus bias dependence shows that **PFBT-Br**, **PFBT-BAr$^F_4$**, and **PFBT-Pr** exhibit a space charged transport regime ($J \propto V^2$) followed by a trap filled regime ($J \propto V^m$, $m > 2$); see Figure 6b for **PFBT-Br**.[31] It is possible to extract hole mobilities from the SCLC region (see eq 2 in the Experimental Section). From these results, one finds hole mobilities (in cm$^2$/V·s) of 3.4 × 10$^{-4}$, 1.1 × 10$^{-5}$, and 6.5 × 10$^{-6}$ for **PFBT-Br**, **PFBT-BAr$^F_4$**, and **PFBT-Pr**, respectively. Thus, hole mobility for **PFBT**-Br is over 1 order of magnitude larger than that for **PFBT-BAr$^F_4$**. These data, together with the optical data previously discussed, support our hypothesis that large CAs act as spacers that separate the polymer chains, thus reducing the polymer chain aggregation, increasing the solid PL quantum yield, and decreasing the charge carrier mobility. That the neutral polymer displays the lowest mobility was unexpected. Perhaps the charged conjugated chains are more extended due to charge repulsion and/or there is better interchain coupling as a result of the aggregation in the polar solvent. Despite these uncertainties, it is interesting to note that the presence of ionic groups does not adversely affect electronic properties and that the charge mobilities can be modulated, for a given conjugated polyelectrolyte backbone, by specifying the electronic coupling/interactions between chains via choice of

(27) (a) Andersson, M.; Rasmark, P. J.; Elvingson, C.; Hansson, P. *Langmuir* **2005**, *21*, 3773. (b) Wang, C.; Tam, K. C. *J. Phys. Chem. B* **2004**, *108*, 8976. (c) Anthony, O.; Zana, R. *Langmuir* **1996**, *12*, 3590.

(28) (a) Salomon, A.; Cahen, D.; Lindsay, S.; Tomfohr, J.; Engelkes, V. B.; Frisbie, C. D. *Adv. Mater.* **2003**, *15*, 1881. (b) Zhang, M.; Hu, Z.; He, T. *J. Phys. Chem. B* **2004**, *108*, 19198. (c) Graaf, H.; Michaelis, W.; Schnurpfeil, G.; Jaeger, N.; Schlettwein, D. *Org. Electron.* **2004**, *5*, 237. (d) Pingree, L. S. C.; Hersam, M. C.; Kern, M. M.; Scott, B. J.; Marks, T. J. *Appl. Phys. Lett.* **2004**, *85*, 344. (e) Ionescu-Zanetti, C.; Mechler, A.; Carter, S. A.; Lal, R. *Adv. Mater.* **2004**, *16*, 385. (f) Nahum, E.; Ebenstein, Y.; Aharoni, A.; Mokari, T.; Banin, U.; Shimoni, N.; Millo, O. *Nano Lett.* **2004**, *4*, 103. (g) Lin, H.-N.; Lin, H.-L.; Wang, S.-S.; Yu, L.-S.; Perng, G.-Y.; Chen, S.-A.; Chen, S.-H. *Appl. Phys. Lett.* **2002**, *81*, 2572. (h) Kelley, T. W.; Frisbie, C. D. *J. Phys. Chem. B* **2001**, *105*, 4538. (i) Loiacono, M. J.; Granstrom, E. L.; Frisbie, C. D. *J. Phys. Chem. B* **1998**, *102*, 1679.

(29) According to the redox onset potentials of cyclic voltammograms measurements recorded at a scan rate of 50 mV/s for the polyelectrolytes cast on a glassy carbon working electrode. The potentials are measured relative to a $Ag^+$/AgCl reference electrode. The onset potential of oxidation process of **PFBT-Br** and $BAr^F_4$ is about 1.4 V.

(30) Parker, I. D. *J. Appl. Phys.* **1994**, *75*, 1656.

(31) Similar $J(V)$ characteristics have been observed in neutral conjugated polymers: (a) Ma, D.; Hummelgen, I. A.; Hu, B.; Karasz, F. E. *J. Appl. Phys.* **1999**, *86*, 3181. (b) Ma, D.; Hummelgen, I. A.; Hu, B.; Karasz, F. E. *J. Phys. D: Appl. Phys.* **1999**, *32*, 2568. (c) Nazeer, K. P.; Jacob, S. A.; Thamilselvan, M.; Mangalaraj, D.; Narayandass, S. K.; Yi, J. *Polym. Int.* **2004**, *53*, 898. (d) Tagmouti, S.; Oueriagli, A.; Outzourhit, A.; Khaidar, M.; Ameziane, E. L.; Yassar, A.; Youssoufi, H. K.; Garnier, F. *Synth. Met.* **1997**, *88*, 109.

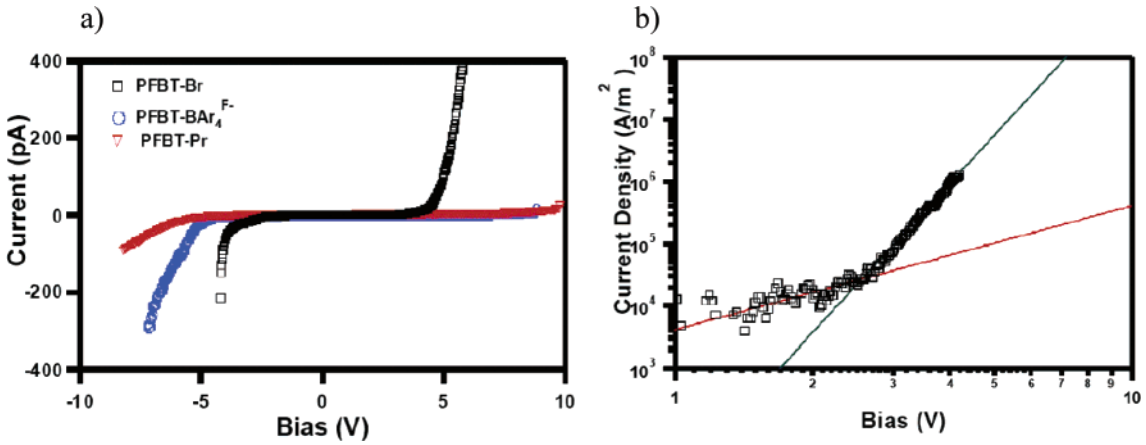


***Figure 6.*** (a) Average $I-V$ curves for **PFBT-Br** (black), **PFBT-BAr$^F_4$** (blue), and **PFBT-Pr** (red) and (b) the current density versus bias for **PFBT-Br**. Solid lines are fits to the SCLC with shallow traps model (see Experimental Section).

CA. Learning how to control these interactions should enable tuning the optical and electrical functions of conjugated polyelectrolytes in specific applications.

CAs also influence charge injection barriers (Figure 6a). The turn-on voltages in forward bias are −3.5 and −5 V for **PFBT-Br** and **PFBT-BAr$^F_4$**, respectively. The lower turn-on voltage and the observable reverse bias current (charge injection from the ITO side) of the **PFBT-Br** film, relative to **PFBT-BAr$^F_4$**, may be attributed to the nature of the surface dipole or differences in HOMO levels that lead to better energy alignment with the ITO work function. Cyclic voltammetry measurements on **PFBT-Br** and **PFBT-BAr$^F_4$** films show no change in the HOMO levels; this rules out the latter possibility. The interface dipole may be due to the migration and accumulation of ions at the electrode surface under the applied electric field[32] and/or the polarization/orientation of the ions at the electrodes. The bromide ions should migrate more rapidly due to their compact size (MW = 79.9 g/mol), as compared to the BAr$^F_4$ ions (MW = 863.3 g/mol). It is also possible that the formation of the interface dipole by $Br^-$ is more effective than that by BAr$^F_4{}^-$, because the charge is more diffuse in the larger CA. We note that reducing the charge injection barrier in organic LEDs by interface dipoles is well documented.[33]

## Conclusion

In summary, a simple protocol is provided for exchanging the charge compensating ions in conjugated polyelectrolytes. This method was demonstrated with **PFBT**, but should prove equally effective for other cationic and anionic conjugated polyelectrolytes. Straightforward characterization of the CA content can be achieved by XPS analysis. We have also shown that the CA influences important properties in solution and in the bulk. For example, the solid-state Φ values can be varied by close to an order of magnitude, with larger anions giving higher yields. We propose that increasing the average interchain distance leads to decreased levels of PL self-quenching. Light scattering studies show that the aggregate particle size in solution can be increased or reduced by the CA. In the case of **PFBT-BAr$^F_4$**, the driving force for aggregation is significantly reduced and the single chain limit is approached. One possible explanation is that the BAr$^F_4$ anion not only balances charge but also associates with the polymer backbone and reduces the driving force for packing as a result of hydrophobic contacts with water. It is interesting that polyelectrolyte theories based exclusively on electrostatic interactions do not provide accurate guidelines to account for these observations.

We also include the first comparison of how the charge compensating ions of conjugated polyelectrolytes influence charge carrier mobility and charge injection barriers. It is significant to note that the presence of the ionic component does not negatively impact charge transport mobility. Indeed, the mobilities are higher for **PFBT-Br** and **PFBT-BAr$^F_4$** when compared to the close structural analogue **PFBT-Pr**, despite possible expectations that the ions may behave as traps for the charge carriers. The higher mobility for **PFBT-Br**, relative to **PFBT-BAr$^F_4$**, may be accounted for by the tighter interchain contacts that result with the smaller ion. Both charge transport measurements and PL efficiencies provide a consistent picture. Charge injection barriers are very strongly perturbed by the CA. Specifically, we have observed both forward and reverse bias injection only with **PFBT-Br**. The exact mechanism for this process is poorly understood. For example, it is not clear to what extent the dipoles organize at the surface or how the charge density of the ionic pair influences the interaction with the metal electrode. Despite these mechanistic uncertainties, the ionic component in conjugated polyelectrolytes provides a versatile structural handle to fine-tune properties relevant to optoelectronic applications, a fact that has not been widely recognized previously.

## Experimental Section

**General Details.** All commercial chemical reagents were obtained from Aldrich and used as received. $^1$H NMR spectra were collected on a Varian Unity Inova 400 MHz spectrometer. UV−vis absorption spectra were recorded on a Shimadzu UV-2401 PC diode array spectrometer. Fluorescence was measured by using a PTI Quantum Master fluorometer. Gel permeation chromatography (GPC) measure-

(32) deMello, J. C. *Phys. Rev. B* **2002**, *66*, 2352105.
(33) (a) Ishii, H.; Sugiyama, K.; Ito, E.; Seki, K. *Adv. Mater.* **1999**, *11*, 605. (b) de Boer, B.; Hadipour, A.; Mandoc, M. M.; van Woudenbergh, T.; Blom, P. W. M. *Adv. Mater.* **2005**, *17*, 621. (c) Campbell, I. H.; Rubin, S.; Zawodzinski, T. A.; Kress, J. D.; Martin, R. L.; Smith, D. L. *Phys. Rev. B* **1996**, *54*, 14321. (d) Hill, I. G.; Rajagopal, A.; Kahn, A.; Hu, Y. *Appl. Phys. Lett.* **1998**, *73*, 662. (e) Hill, I. G.; Makinen, A. J.; Kafafi, Z. H. *J. Appl. Phys.* **2000**, *88*, 889. (f) Peisert, H.; Knupfer, M.; Schwieger, T.; Auerhammer, J. M.; Golden, M. S.; Fink, J. *J. Appl. Phys.* **2002**, *91*, 4872. (g) Brown, T. M.; Friend, R. H.; Millard, I. S.; Lacey, D. J.; Butler, T.; Burroughes, J. H.; Cacialli, F. *J. Appl. Phys.* **2003**, *93*, 6159. (h) Koch, N.; Kahn, A.; Ghijsen, J.; Pireaux, J.-J.; Schwartz, J.; Johnson, R. L.; Elschner, A. *Appl. Phys. Lett.* **2003**, *82*, 70. (i) Wu, H.; Huang, F.; Mo, Y.; Yang, W.; Wang, D.; Peng, J.; Cao, Y. *Adv. Mater.* **2004**, *16*, 1826.

ments were done in a Waters GPC 2410 in tetrahydrofuran (THF) via a calibration curve of polystyrene standards. Dynamic light scattering (DLS) was recorded using 10 mW HeNe laser (wavelength 633 nm) with a photodiode detector BI-APD (Brookhaven Instruments Co.). The synthesis of **PFBT-Br** was adapted from the literature.[7]

**Poly[9,9-bis(6′-bromohexyl)fluorene-*alt*-4,7-(2,1,3-benzothiadiazole)].** Carefully purified 2,7-bis(4,4,5,5-tetramethyl-1,3,2-dioxaborolan-2-yl)-9,9-bis(6′-bromohexyl)fluorene (0.5 mmol, 372 mg), 4,7-dibromo-2,1,3-benzothiadiazole (0.5 mmol, 147 mg), and $Pd(PPh_3)_4$ (10 mg) were dissolved in a mixture of toluene and aqueous 2 M $Na_2CO_3$. The solution was refluxed with vigorous stirring for 36 h under an argon atmosphere. The mixture was then poured into methanol. The precipitated material was recovered by filtration and washed for 3 h by stirring in acetone to remove oligomers and catalyst residues. The resulting solids were air-dried overnight, followed by drying under vacuum to afford **PFBT** precursor as 224 mg (72%) of a bright yellow powder. GPC analysis gave $M_n = 22\,500$ and PDI = 1.8. $^1$H NMR (400 MHz, $CDCl_3$), $\delta$ (ppm): 8.10−7.68 (m, 8H), 3.28 (m, 4H), 2.10 (m, 4H), 1.68 (m, 4H), 1.30−1.12 (m, 8H), 0.89−0.75 (m, 4H).

**Poly[(9,9-bis(6′-*N*,*N*,*N*-trimethylammoniumbromide)hexyl)fluorene-*alt*-4,7-(2,1,3-benzothiadiazole)] (PFBT-Br).** Condensed trimethylamine (2.5 mL) was added dropwise to a solution of the neutral precursor polymer (100 mg) in tetrahydrofuran (10 mL) at −78 °C. The mixture was allowed to warm to room temperature gradually. The precipitate was redissolved by addition of excess water, and then an extra 2 mL of trimethylamine was added at −78 °C, and the mixture was stirred vigorous for 24 h at room temperature. After removal of most of the water under reduced pressure, acetone was added to precipitate the cationic polymer, which was collected and dried in a vacuum oven to give 101 mg (85%) of **PFBT-Br** as a powder. $^1$H NMR (400 MHz, DMSO-$d_6$), $\delta$ (ppm): 8.30−7.97 (m, 8H), 3.36 (m, 4H), 3.22 (br, 4H), 2.98 (s, 18H), 1.53 (br, 4H), 1.14 (br, 8H), 0.84 (br, 4H).

**General Anion Exchange Procedure.** Poly[(9,9-bis(6′-*N*,*N*,*N*-trimethylammonium bromide)hexyl)fluorene-*alt*-4,7-(2,1,3-benzothiadiazole)] (**PFBT-Br**), 56 mg (0.075 mmol in repeat units), was dissolved in 10 mL of methanol. Subsequently, a solution of the corresponding salt (0.45 mmol) in 10 mL of water and/or methanol was added. The mixture was stirred for 2 days at room temperature. After removal of methanol under reduced pressure, deionized water was added several times to wash the residue. The overall procedure can be repeated until the majority of the bromide is removed. Finally, the resulting polymer was dried under vacuum.

**Poly[(9,9-bis(6′-*N*,*N*,*N*-trimethylammonium)hexyl)fluorene-*alt*-4,7-(2,1,3-benzothiadiazole)] Tetrafluoroborate (PFBT-$BF_4$).** **PFBT-Br**, 56 mg (0.075 mmol), and sodium tetrafluoroborate, 50 mg (0.45 mmol), were used to obtain 39 mg (69%) of **PFBT-$BF_4$**. $^1$H NMR (400 MHz, DMSO-$d_6$), $\delta$ (ppm): 8.28−7.94 (m, 8H), 3.36 (m, 4H), 3.12 (br, 4H), 2.93 (s, 18H), 1.48 (br, 4H), 1.16−1.05 (m, 8H), 0.78 (br, 4H).

**Poly[(9,9-bis(6′-*N*,*N*,*N*-trimethylammonium)hexyl)fluorene-*alt*-4,7-(2,1,3-benzothiadiazole)] Trifluoromethanesulfonate (PFBT-$CF_3SO_3$).** **PFBT-Br**, 56 mg (0.075 mmol), and sodium trifluoromethanesulfonate, 77 mg (0.45 mmol), were used to yield 47 mg (71%) of **PFBT-$CF_3SO_3$.** $^1$H NMR (400 MHz, DMSO-$d_6$), $\delta$ (ppm): 8.30−7.90 (m, 8H), 3.34 (m, 4H), 3.11 (br, 4H), 2.93 (s, 18H), 1.50 (br, 4H), 1.14 (br, 8H), 0.82 (br, 4H).

**Poly[(9,9-bis(6′-*N*,*N*,*N*-trimethylammonium)hexyl)fluorene-*alt*-4,7-(2,1,3-benzothiadiazole)] Hexafluorophosphate (PFBT-$PF_6$).** **PFBT-Br**, 56 mg (0.075 mmol), and ammonium hexafluorophosphate, 73 mg (0.45 mmol), were used to yield 49 mg (75%) of **PFBT-$PF_6$**. $^1$H NMR (400 MHz, DMSO-$d_6$), $\delta$ (ppm): 8.25−7.82 (m, 8H), 3.37 (m, 4H), 3.12 (br, 4H), 2.93 (s, 18H), 1.50 (br, 4H), 1.14 (br, 8H), 0.81 (br, 4H).

**Poly[(9,9-bis(6′-*N*,*N*,*N*-trimethylammonium)hexyl)fluorene-*alt*-4,7-(2,1,3-benzothiadiazole)] Tetraphenylborate (PFBT-$BPh_4$).** **PFBT-Br**, 56 mg (0.075 mmol), and ammonium tetraphenylborate, 152 mg (0.45 mmol), were used to yield 67 mg (73%) of the target product. $^1$H NMR (400 MHz, DMSO-$d_6$), $\delta$ (ppm): 8.25−7.92 (m, 8H), 7.18 (s, 16H), 6.91 (t, 16H, $J = 7.2$ Hz), 6.77 (t, 8H, $J = 7.2$ Hz), 3.36 (m, 4H), 3.07 (br, 4H), 2.87 (s, 18H), 1.45 (br, 4H), 1.15 (br, 8H), 0.83 (br, 4H).

**Poly[(9,9-bis(6′-*N*,*N*,*N*-trimethylammonium)hexyl)fluorene-*alt*-4,7-(2,1,3-benzothiadiazole)] Tetrakis[3,5-bis(trifluoromethyl)phenyl]borate (PFBT-$BAr^F_4$).** **PFBT-Br**, 19 mg (0.026 mmol), and sodium tetrakis[3,5-bis(trifluoromethyl)phenyl]borate, 50 mg (0.056 mmol), were used to obtain 44 mg (73%) of **PFBT-$BAr^F_4$**. $^1$H NMR (400 MHz, DMSO-$d_6$), $\delta$ (ppm): 8.27−7.98 (m, 8H), 7.70 (s, 8H), 7.61 (s, 16H), 3.36 (m, 4H), 3.12 (br, 4H), 2.93 (s, 18H), 1.47 (br, 4H), 1.13 (br, 8H), 0.84 (br, 4H).

**X-ray Photoelectron Spectroscopy Analysis.** XPS spectra were recorded on a Kratos Axis Ultra XPS system with a base pressure of $1 \times 10^{-10}$ mbar (UHV), using a monochromated Al Kα X-ray source at $h\nu = 1486$ eV. Polymer samples were placed on one side of a double-sided carbon adhesive. The measured binding energy (BE) of C1s was referenced to 284.5 eV. The two peaks located at a binding energy of about 99 and 149 eV were assigned to Si2p and Si2s of the carbon adhesive. When the sample film was thinner, the two peaks of Si element were higher. The original polymer containing Br anion (**PFBT-Br**) showed four distinct characteristic peaks of Br atom (Figure 1), Br3d, $Br3p_{3/2}$, $Br3p_{1/2}$, and Br3s, located at binding energies of 69, 182, 189, and 257 eV, respectively. The peak at 532 eV of O1s originated from water in polymer. In the XPS spectra of polyelectrolyte exchanged Br with different anions, the Br peaks nearly disappeared, and the corresponding exchange ions' elemental characteristic peaks were recorded. For **PFBT-$BF_4$**, the F1s and F2s located at 686 and 30 eV, respectively, and the B1s peak appeared at 192 eV, a little higher than the normal value because of fluoro atoms around boron (Figure S1). For **PFBT-$CF_3SO_3$**, F1s appeared at 687 eV, and S2p has four peaks (163, 164, 166, and 167 eV), corresponding to two different chemical environments of sulfur atoms (Figure S2). For **PFBT-$PF_6$**, F1s, F2s, and P2p were located at 686, 31, and 135 eV, respectively (Figure S3). For **PFBT-$BPh_4$**, B1s appeared at 187 eV (Figure S4). For **PFBT-$BAr^F_4$**, F1s, F2s, and B1s were located at 687, 31, and 188 eV, respectively (Figure 2). Atomic concentration ratios calculated from peak intensities using CasaXPS Version 2.3.5 software[34] revealed greater than 95% bromide exchange.

**Scanning Probe Measurements.** All measurements were done under ambient conditions and in the dark using a commercial scanning probe microscope (MultiMode equipped with CAFM module and the Nanoscope Controller IIIa, Veeco Inc.). Platinum-coated Si tips with a spring constant of 0.2 N/m and a tip radius of 25 nm were used (Budget Sensors). In these measurements, the conducting probe makes contact with the sample (the tip acts as a nanoelectrode) and measures current as a function of applied voltage either at certain points on a surface ($I-V$ curve) or map out a current image at a fixed bias. The bias was applied to the conducting substrate, and the current was measured by a preamplifier. For each sample, the $I-V$ curves and topographic images were collected on multiple locations to examine the film uniformity.

Polymer films were cast onto an ITO-coated glass substrate from methanol solutions ($3.42 \times 10^{-3}$ M in polymer repeat units). The film thickness was 18 nm for **PFBT-Br** and 20 nm for **PFBT-$BAr^F_4$** as measured by ellipsometry and by AFM. Subsequently, the probe tip was used to measure current across the film with a tip−sample contact area of 84 nm$^2$ using the Hertz model.[35] The bias was applied to the conducting substrate. The same tip and applied contact force (40 nN) were used to obtain the $I-V$ curves for all samples to ensure identical

(34) Scofield, J. H. *J. Electron Spectrosc. Relat. Phenom.* **1976**, *8*, 129.
(35) From the Hertz model, the contact radius, $a$, is described by: $a = (3FR/4Y^*)^{1/3}$ and $1/Y^* = (1 - \nu_1^2)/Y_1 + (1 - \nu_2^2)/Y_2$, where $F$ is the load, $R$ is the tip radius, $Y$ is Young's modulus, and $\nu$ is Poisson's ratio. With $F =$ 40 nN, $R = 25$ nm, $Y_1 = 168$ Gpa, and $\nu_1 = 0.38$ for Pt, $Y_2 = 3$ GPa and $\nu_2 = 0.35$ for polymer, and $a$ is calculated to be around 6.03 nm.

contact resistance. To test the tip quality, the $I-V$ curves of the ITO or gold substrate were collected before and after the $I-V$ curves at each location were measured. The data and the tip were discarded whenever the current decreased, a sign of a damaged or worn tip. To prolong tip lifetime, samples were imaged in tapping mode, and then $I-V$ curves were collected at selected points in contact mode.

**Analysis of C-AFM Data.** It is well-accepted that the charge transport for most conjugated polymers is dominated by a thermally activated hopping mechanism in which carriers hop across barriers created by the presence of isolated states or domains.[36] The space charge limiting current (SCLC) conduction model can often be used to describe the current−voltage characteristics of electrons or holes in these materials due to the low charge carrier mobility. Under these conditions, the current density, $J$, can be described by the trap-free Mott−Gurney law:[37]

$$J = \frac{9}{8}\epsilon_r\epsilon_o\mu\frac{V^2}{L^3} \tag{1}$$

where $\epsilon_r$ is the dielectric constant of the polymer, $\epsilon_o$ is the vacuum permittivity, $\mu$ is the charge mobility, $V$ is the applied voltage, and $L$ is the film thickness. When the current−voltage follows a square-law dependence, the charge process is thus trap-free space charge limited. If the current−voltage follows a power-law dependence ($J \propto V^m$ with $m > 2$), the charge transport process is trap-dependent. Generally, a transition from $J \propto V^1$ (ohmic) at low voltages to $J \propto V^2$ (space-charge-limited) to $J \propto V^m$, $m > 2$ (trapped filling), at high voltages indicates the presence of shallow traps, whereas a direct transition from $J \propto V^1$ to $J \propto V^m$ indicates the presence of deep traps.[38] SCLC in the presence of single discrete energy level traps is described by:[39]

$$J = \frac{9}{8}\epsilon_r\epsilon_o\theta\mu\frac{V^2}{L^3} \tag{2}$$

with

$$\theta = \frac{n}{n + n_t}$$

or

$$\theta = \frac{p}{p + p_t}$$

for electron and hole, respectively. In eq 2, $n$ is the density of free electrons, $n_t$ is the density of trapped electrons, $p$ is the density of free holes, and $p_t$ is the density of trapped holes. Experimentally, $\theta$ is determined from the ratio of $J$ at the beginning and at the end of the $J \propto V^2$ region: $\theta = J_{min}/J_{max}$. For eq 2 to apply, the charge mobility has to be independent or weakly dependent on the electric field.

**Acknowledgment.** We are grateful to the Mitsubishi Chemical Center for Advanced Materials (MC-CAM) at UCSB for financial support. T.-Q.N. acknowledges the support from the ONR Young Investigator Program and the University of California. A.G. is the recipient of a Graduate Opportunity Fellowship provided by UCSB. We benefited from stimulating discussions with Drs. Bin Liu, Han Young Woo, and Hongbin Wu.

**Supporting Information Available:** X-ray photoelectron spectroscopy (XPS) analysis and Figures S1−6. This material is available free of charge via the Internet at http://pubs.acs.org.

JA0611341

(36) (a) Bassler, H. *Phys. Status Solidi B* **1993**, *175*, 15. (b) Novikov, S. V.; Dunlap, D. H.; Kenkre, V. M.; Parris, P. E.; Vannikov, A. V. *Phys. Rev. Lett.* **1998**, *81*, 4472. (c) Rakhmanova, S. V.; Conwell, E. M. *Synth. Met.* **2001**, *116*, 389.

(37) Mott, N. F.; Gurney, R. W. *Electronic Processes in Ionic Crystals*; Oxford University Press: London, 1948.

(38) (a) Lampert, M. A. *Rep. Prog. Phys.* **1964**, *27*, 329. (b) Lampert, M. A.; Mark, P. *Current Injection in Solids*; Academic Press: New York, 1970.

(39) (a) Lampert, M. A. *Phys. Rev.* **1956**, *103*, 1648. (b) Kao, K. C.; Hwang, W. *Electrical Transport in Solids*; Pergamon: New York, 1981.